J. Phys.: Condens. Matter 3 (1991) 8945–8957. Printed in the UK

Polarized charge transfer spectra of Cu^{2+} doped TMA_2MnCl_4 crystals: study of the $CuCl_4^{2-}$ Jahn–Teller distortion

M C Marco de Lucas, F Rodríguez and J A Aramburu
DCITTYM (Sección Ciencia de Materiales), Facultad de Ciencias, Universidad de Cantabria, 39005 – Santander, Spain

Received 19 March 1991, in final form 13 June 1991

Abstract. The charge transfer (CT) spectra of the $CuCl_4^{2-}$ complex formed in $TMA_2MnCl_4:Cu^{2+}$ single crystals are investigated in the 10–300 K temperature range. Two x,y-polarized bands at 24 300 and 33 700 cm^{-1}, and two z-polarized ones at 29 500 and 41 000 cm^{-1} are assigned to CT transitions of the $CuCl_4^{2-}$. These transition energies, as well as the degree of polarization of the CT bands, are explained in terms of Jahn–Teller distortions of D_{2d} symmetry. The MS-Xα calculations performed on this complex support this view. By means of these data, both the trans-Cl–Cu–Cl distortion angle and the orientation of $CuCl_4^{2-}$ in the lattice are determined.

The sensitivity of CT bands of $CuCl_4^{2-}$ for detecting the structural phase transition sequence of this crystal is analysed as well. A noteworthy finding of this work concerns the profound changes experienced by CT bands below the monoclinic $P112_1/n \rightarrow P12_1/c1$ phase transition temperature at 171 K. The spectra become nearly isotropic as a consequence of the formation of structural domains.

These results are compared with those obtained in pure chlorocuprates such as Cs_2CuCl_4 and TMA_2CuCl_4.

1. Introduction

There has been particular interest in CuX_n complexes (X = halogen ion, $n = 4$, 6, and Cu as divalent cation). These basic systems present the simplest electronic configuration (d^9) among transition metal ion complexes, and their optical transitions involve simple electronic jumps between one-electron molecular orbitals (MO). The optical absorption spectra of these Cu^{2+} complexes in the crystal field (CF) and charge transfer (CT) regions strongly depend not only on the symmetry and degree of the Jahn–Teller distortion displayed by the Cu^{2+} ligands but also on the orientation of the CuX_n in the lattice. This dependence has been extensively studied in pure chlorocuprate (II) compounds where the local structure around the Cu^{2+} is well known from x-ray diffraction techniques [1, 2]. In tetracoordinated A_2CuCl_4 crystals, it has been found that $CuCl_4^{2-}$ complexes usually present Jahn–Teller distortions of nearly D_{2d} symmetry. A large number of crystals of this type has been synthesized and the transition energies and polarization type of the CF bands have been correlated with the trans-Cl–Cu–Cl distortion angle from about 125° to 180° (D_{4h} square planar complex) of the $CuCl_4^{2-}$ with different Cu^{2+}–Cl^- distances, ranging from 2.21 to 2.27 Å [1–4]. However, such correlations have been less

0953-8984/91/458945 + 13 $03.50

studied for CT transitions. The high oscillator strengths of these CT transitions (~0.1) [5], two or three orders of magnitude greater than those of the corresponding CF transitions [6], make it difficult to obtain reliable spectra in this CT region.

Although attempts have been made to detect CT spectra in cesium compounds by using thin layers of Cs_2CuCl_4 crystals [7, 8], reflectance spectroscopy [5] or by diluting $CuCl_4^{2-}$ in transparent matrices like Cs_2ZnCl_4 [5, 8, 9], the strong absorption backgrounds observed in the UV region precluded accurate measurement of the absorption intensities and only qualitative information about band polarization was obtained from such spectra.

The $CuCl_4^{2-}$ CT band assignment in Cs_2CuCl_4 and $Cs_2ZnCl_4:Cu^{2+}$ has been carried out through several Xα calculations on the pseudotetrahedral $CuCl_4^{2-}$ complex (D_{2d} geometry) [5, 10–13]. Nevertheless, the first MS-Xα calculations performed by Desjardins *et al* [5] and Bencini and Gatteschi [10], predict CT transition energies which are greatly shifted (more than 30%) from the experimental values. Later MS-Xα calculations by Gewirth *et al* [11, 12], improve the previous results by about 15% though the procedure used leads to unusual values of the copper and chlorine spheres radii as discussed below. Recent DV-Xα calculations on this complex by Deeth [13] are also discussed.

In this work, the CT spectra of $CuCl_4^{2-}$ complexes formed in TMA_2MnCl_4 (TMA = $(CH_3)_4N$) single crystals were investigated in the 10–300 K temperature range. This crystal was chosen for the following reasons: (1) the easy substitution of Cu^{2+} for Mn^{2+} ions allowed us to dope the crystals with optimum Cu^{2+} concentrations for obtaining reliable CT spectra. The significant backgrounds observed in previous crystals were greatly reduced in the present case, and therefore, precise measurements of the integrated band intensities were possible; (2) this crystal provides a well known sequence of structural phase transitions which has been investigated by means of different experimental techniques [14–21]. These phase transitions have recently been studied in the 10–300 K temperature range through the optical spectra of tetrahedral $MnCl_4^{2-}$ complexes in the pure crystal [20, 21].

The optical absorption spectra of $TMA_2MnCl_4:Cu^{2+}$ and the new MS-Xα calculations on the D_{2d} $CuCl_4^{2-}$ complex that are presented in this work allow us to make a clearer CT band assignment. The correlation between experimental and theoretical results, and the polarization of these CT bands also provide useful information about the degree of distortion of $CuCl_4^{2-}$ and about how they are oriented within the lattice, respectively.

The sensitivity of CT bands as local probes for detecting the structural phase transitions in this crystal is also analysed. This aspect was recently investigated in mixed $NH_4Cl_{1-x}Br_x$ and pure ammonium halide crystals doped with Cu^{2+} [22–24]. These studies showed that CT bands are sensitive enough to detect not only the different types of phase transitions displayed by this family of crystals but also the displacive effects associated with the small first-order character accompanying the λ transition in NH_4Cl at $T = 242$ K, which involves changes in the lattice parameter of only 0.005 Å.

2. Experimental details

Single crystals of $CuCl_2$-doped TMA_2MnCl_4 were grown by slow evaporation at 30 °C of acidic aqueous solutions containing stoichiometric amounts of $N(CH_3)_4Cl$ and $MnCl_2 \cdot 4H_2O$, and different $CuCl_2$ concentrations from 0.01 to 0.1 mol%. The orthorhombic crystallographic structure (*Pmcn* space group) at 300 K and the crystal orientation were checked by x-ray diffraction techniques. Several *b*- and *a*-plates of good

optical quality with sizes of about $1 \times 1 \times 0.3$ mm^3 were selected and polished for the optical studies. The real Cu^{2+} concentration of these crystals was measured by atomic absorption spectroscopy.

Polarized optical absorption spectra were recorded on a Lambda 9 Perkin Elmer spectrophotometer equipped with Glan Taylor polarizing prisms. The temperature was stabilized to within 0.05 K in the 10–300 K range with a Scientific Instruments 202 closed circuit cryostat and an APD-K controller.

Extinction directions and their temperature dependence were observed through a polarizing microscope.

3. Theoretical details

The standard version of the SCF-MS-Xα method [25] was used to carry out spin–restricted calculations on the D_{2d} $CuCl_4^{2-}$ cluster. Two $CuCl_4^{2-}$ geometries have been worked out: (1) metal–ligand distance $R = 2.230$ Å and the trans-Cl–Cu–Cl angle $\theta = 129.2°$(Cs_2CuCl_4) [26, 27]; (2) $R = 2.230$ Å and $\theta = 120°$.

Neutral atoms have been used in the initial atomic calculation to construct the starting molecular potential. The sphere radii of the muffin-tin approximation were determined following completely the Norman's procedure [28]: (1) the ratio of the sphere radii, r, was fixed to the ratio of the 'atomic number radii'; (2) we allowed the atomic spheres to overlap; (3) the absolute values of the radii have been determined by imposing a virial ratio, $v_r = -2\langle T\rangle/\langle V\rangle$, to be exactly one. In the present calculations, v_r was kept to be better than 1.000 001. The use of this criterium, in previous calculations carried out on copper complexes [29, 30], led to accurate values (within 2000 cm^{-1}) of the CT transition energies.

The values of the sphere radii obtained in $CuCl_4^{2-}$ with $\theta = 129.2°$ following this procedure are $\rho(Cu) = 1.31$ Å and $\rho(Cl) = 1.56$ Å. Such values correspond to an overlap volume of each chlorine sphere of 5.5% and a ratio of sphere radii $r = \rho(Cl)/\rho(Cu) = 0.84$.

Electronic transition energies were calculated using the transition state procedure.

4. Results

Figure 1 shows the $T = 300$ K optical absorption spectra in the 220–500 nm range of Cu^{2+}-doped TMA_2MnCl_4 single crystals with incident light polarized along the ***a***, ***b*** and ***c*** orthorhombic directions (hereafter called ***a***, ***b*** and ***c***). Three prominent anisotropic absorption bands, denoted by A, B and C, are clearly seen at 24 300, 33 700 and 41 000 cm^{-1}, respectively. A and B display the same polarization and have maximum and minimum intensities along the ***a*** and ***b*** directions, respectively, while the opposite behaviour is observed for the C band. One shoulder, C', located at about 29 500 cm^{-1}, is also observed near the B band in the spectra of figure 1 with a dominant polarization as the C band. These bands are associated with the presence of Cu^{2+}, as their intensities are proportional to the Cu^{2+} concentration.

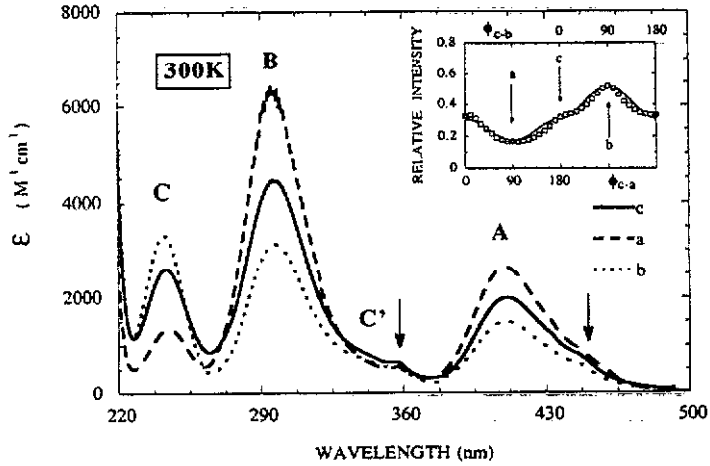

Figure 1. Polarized optical absorption spectra of $TMA_2MnCl_4:Cu^{2+}$ at $T = 300$ K. (010) and (100) single crystal plates were used for obtaining the *a*, *b* and *c* polarizations. Spectra were taken with *E* parallel to *a* and *c* on the (010) single crystal plate, and with *E* parallel to *b* and *c* on the (100), respectively. The spectra with *E* parallel to *c* are the same in both crystals. The arrows indicate the location of Mn^{2+} crystal field peaks. The inset shows dependence of the C band intensity on the polarization angle, φ, which is the angle *E* makes with *c*: (□) experimental points. Full curve depicts the functions given in equation (5). The Cu^{2+} concentration was 4200 ppm.

The relative band intensity, Ir_i, for each polarization $i = a, b$ and c, was calculated for the three bands through the equation

$$Ir_i = I_i \Big/ \sum_{j=a,b,c} I_j \tag{1}$$

where I_i and I_j represent the integrated band intensities along the i and j directions, respectively. The Ir_i values derived from the spectra of figure 1 are 0.44, 0.23, 0.33 for the A band; 0.45, 0.24, 0.31 for B; and 0.16, 0.51, 0.33 for C, along *a*, *b* and *c*, respectively. These values are characteristic of the crystals and they do not depend on the crystal growing conditions or on the Cu^{2+} concentration.

The inset of figure 1 portrays the variation of the relative intensity of the C band, Ir^C, with the angles, φ_{c-a} and φ_{c-b}, that the polarization plane makes with the *c* direction in (010) and (100) crystal faces, respectively. The full curve depicts the function $I(\varphi_{c-a}) = 0.31\cos^2\varphi_{c-a} + 0.17\sin^2\varphi_{c-a}$ in (001), and $I(\varphi_{c-b}) = 0.31\cos^2\varphi_{c-b} + 0.52\sin^2\varphi_{c-b}$ in (100).

Upon cooling, no significant changes are observed in the spectra in the 300–171 K temperature range. Only small jumps in the relative intensities, Ir_i, of less than 10% are detected at the structural phase transition temperatures of the TMA_2MnCl_4 crystals: 292.6 K, 292.3 K and 268.7 K ($Pmcn \rightarrow$ incommensurate $\rightarrow P2_1/c11 \rightarrow P112_1/n$). Band narrowings of about 500 cm^{-1} and band shifts of 100 cm^{-1} are measured in this temperature range.

However, the $P112_1/n \rightarrow P12_1/c1$ structural phase transition at 171 K induces abrupt changes in the optical absorption spectra as depicted in figure 2. Besides the band narrowing, these spectra exhibit no further significant modifications down to 10 K (figure

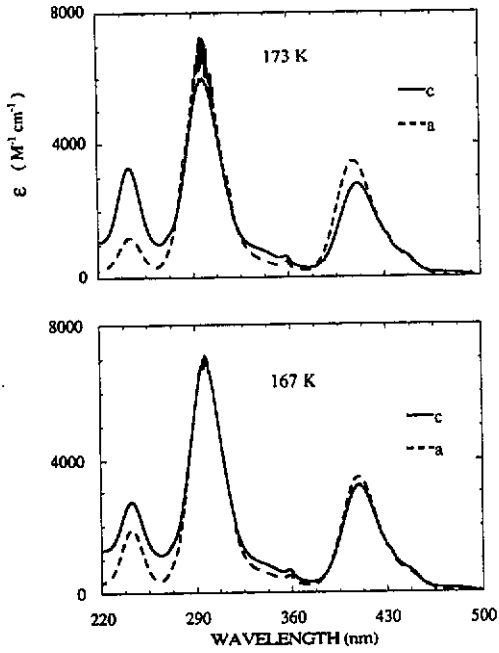

Figure 2. Polarized optical absorption spectra taken with E parallel to a and c on the (010) face of $TMA_2MnCl_4:Cu^{2+}$. The spectra were recorded above ($T = 173$ K) and below ($T = 167$ K) the $P112_1/n \rightarrow P12_1/c1$ structural phase transition at $T = 171$ K.

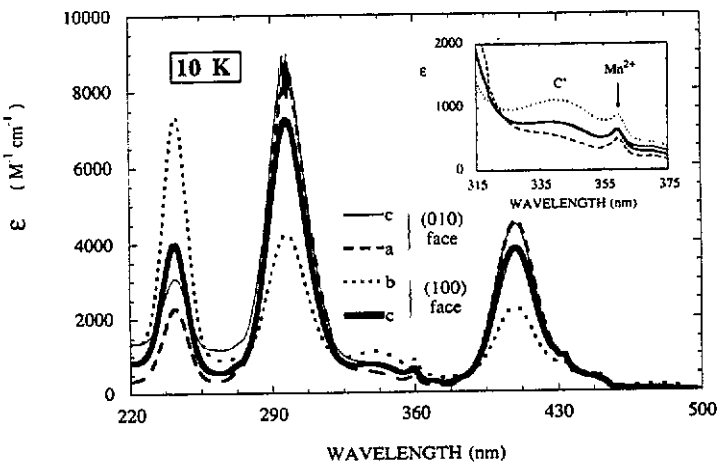

Figure 3. $T = 10$ K polarized optical absorption spectra of $TMA_2MnCl_4:Cu^{2+}$. The inset shows a magnification of the C′ band to clarify its polarization.

3). A noteworthy fact at this temperature concerns the isotropy of the spectrum taken in the (010) plane. The c and a polarized spectra become nearly the same, remaining unchanged with the polarization angle within the (010) plane. However, they are still anisotropes in (100) (c and b polarizations) and the spectrum along c does not correspond to that obtained along c in the (010) plane. The C band intensity in (100) is about twice that observed in (010) while A and B bands have similar intensities in both planes.

At 10 K, the shoulder, C', appears at 29 500 cm^{-1} and, because of the band narrowing, its polarization is now clearer than at 300 K, though no quantitative estimations of Ir_i were made (inset of figure 3).

5. Analysis and discussion

5.1. Polarization analysis: Jahn–Teller distortion and $CuCl_4^{2-}$ orientation

The transition energies and the molar extinction coefficients of the absorption bands A, B and C of the $TMA_2MnCl_4:Cu^{2+}$ crystals are characteristic of CT transitions of Cu^{2+} complexes having Cl^- anions as ligands. Given that Cu^{2+} replaces the tetrahedrally coordinated Mn^{2+}, the complexes involved must be $CuCl_4^{2-}$.

The relative intensities, Ir_i, measured at 300 K, allowed us to conclude that A and B bands are x, y-polarized while C is completely z-polarized, where z is taken along the symmetry axis of the distorted $CuCl_4^{2-}$ complexes.

Independently of the particular orientations of $CuCl_4^{2-}$ and the crystallographic structure of the host matrix, it is easy to identify bands displaying x-, y- or z-polarizations from the Ir_i values, $i = \boldsymbol{a}, \boldsymbol{b}$ and $\boldsymbol{c}$, provided we are dealing with single crystals. In fact, electric dipole allowed transitions which are polarized either along a given z-direction or in the (x, y) perpendicular plane, must verify the following equations:

$$\sum_{i=a,b,c} I_i^z \propto f_1^2 \sum_{i=a,b,c} \cos^2\theta_i = f_1^2$$

$$\sum_{i=a,b,c} I_i^{xy} \propto f_2^2 \sum_{i=a,b,c} \sin^2\theta_i = 2f_2^2. \qquad (2)$$

I_i^z and I_i^{xy} are the total integrated band intensities along the i-direction for z- and x, y-polarized transitions, respectively; f_1 and f_2 are their respective oscillator strengths, and θ_i is the angle z makes with each orthorhombic direction, $i = \boldsymbol{a}, \boldsymbol{b}$ and $\boldsymbol{c}$. Once the values of Ir_i are determined from equation (1), it is possible to distinguish between x-, y- or z-polarizations by taking into account:

$$Ir_i^z + 2Ir_i^{xy} = \cos^2\theta_i + \sin^2\theta_i = 1 \qquad (3)$$

for every direction, $i = \boldsymbol{a}, \boldsymbol{b}$ and $\boldsymbol{c}$.

By inspecting table 1 it follows that A and B are x,y-polarized, while C is z-polarized. Therefore, the C' band is principally z-polarized. Though we confined these calculations to systems with only one z-direction of distortion, the same conclusion applies to systems having different $CuCl_4^{2-}$ orientations.

Except for the C' band, these polarizations were also qualitatively deduced for the CT bands of $CuCl_4^{2-}$ complexes in Cs_2ZnCl_4 and the pure Cs_2CuCl_4 compounds on the basis of D_{2d} symmetry distortions [5–8]. In our case, a similar distortion symmetry is expected for the Cu^{2+} substituted tetrahedral Mn^{2+}. In fact, $CuCl_4^{2-}$ complexes usually display D_{2d}-type distortions corresponding to flattened tetrahedra, at variance with the $CuCl_6^{4-}$ complexes in which D_{4h} elongated [31] (or unusually compressed [29]) octahedral distortions are present. These experimental observations reflect the fact that vibrational modes of e (bending) symmetry in T_d, and those of e_g (stretching) symmetry in O_h complexes, are the most relevant in Jahn–Teller couplings [32].

Consequently, we assume D_{2d} symmetry for the $CuCl_4^{2-}$ complexes formed in TMA_2MnCl_4. This assumption is also supported by the optical absorption spectra of

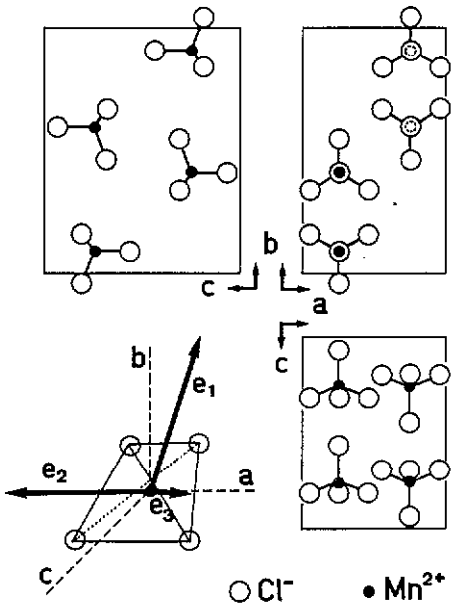

Figure 4. (100), (010) and (001) projections of the TMA_2MnCl_4 unit cell (*Pmcn* space group). Only the four $MnCl_4^{2-}$ units at (4c) sites were drawn. The figure on the left side in the bottom shows the unitary vectors e_1, e_2 and e_3 along the S_4 axes of the $MnCl_4^{2-}$ tetrahedron. $CuCl_4^{2-}$ distortions of D_{2d} symmetry would correspond to a flattened tetrahedron along one of the S_4 axes. The trans-Cl–Cu–Cl angle, θ, equal to 109° for regular tetrahedra, defines the degree of distortion of these $CuCl_4^{2-}$ complexes.

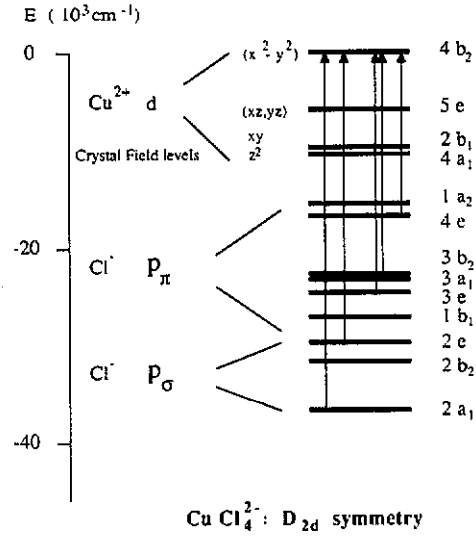

Figure 5. Energy level diagram of the $CuCl_4^{2-}$ complex in D_{2d} symmetry corresponding to the electronic ground state configuration obtained in our MS-Xα calculation (R = 2.230 Å, θ = 129.2°). Energies are given with respect to the $4b_2(x^2 - y^2)$ MO. The arrows indicate the symmetry-allowed electric dipole transitions.

figures 1–3 which resemble the CT spectra of the isomorphous TMA_2CuCl_4 and Cs_2CuCl_4 where the local structure around the Cu^{2+} is known to be nearly D_{2d} [5–8, 26, 33, 34].

The values of Ir_i, equal to $\cos^2\theta_i$ or $(\sin^2\theta_i)/2$ depending on the z- or x,y-polarization of the band, also contain useful information about the $CuCl_4^{2-}$ orientation in TMA_2MnCl_4. When analysing this information it is advantageous to take into account the possible Jahn–Teller distortions on the basis of its *Pmcn* crystallographic structure at 300 K [35]. The unit cell contains four $MnCl_4^{2-}$ units in (4c) sites, with one of the Mn^{2+}–Cl^- bonds along c and the other three Cl^- ions lying in the (001) plane as indicated in figure 4. $MnCl_4^{2-}$ tetrahedra also lie in mirror planes parallel to (100) at $\frac{1}{4}a$ within the unit cell. It is important to point out the existence of a structural disorder in the orthorhombic phase of this family of crystals associated with $MnCl_4^{2-}$ rotations around the c-axis, which has been evidenced by x-ray diffraction [35, 36] and NMR [37–39] techniques.

Jahn–Teller distortions of $CuCl_4^{2-}$ would take place along one of the three S_4 axes of the $MnCl_4^{2-}$ tetrahedron. The square components of the unitary vectors (denoted by e_1, e_2 and e_3) pointing along the three S_4 axes, are the same for the four $MnCl_4^{2-}$ tetrahedra of the unit cell and are given in table 1 together with the $\cos^2\theta_i$-values deduced from the spectra of figure 1.

Table 1. e_1, e_2 and e_3 denote the square components of the unitary vectors e_1, e_2 and e_3 pointing along the S_4 axes of the $MnCl_4^{2-}$ tetrahedra in TMA_2MnCl_4 with respect to the orthogonal a, b and c directions, respectively. Ir_i, with $i = a$, b and c, are the relative intensities of bands A, B and C, defined in equation (1). Last two columns show the polarization type of the bands: xy-type for bands A and B, and z-type for C.

			Relative intensities				
i direction	e_1	$e_2(e_3)$	Ir_i^A	Ir_i^B	Ir_i^C	$Ir_i^C + 2Ir_i^A$	$Ir_i^C + 2Ir_i^B$
a	0	0.50	0.44	0.45	0.16	1.04	1.06
b	0.69	0.16	0.23	0.24	0.51	0.97	0.99
c	0.31	0.34	0.33	0.31	0.33	0.99	0.95

The anisotropy of CT spectra clearly indicates that Jahn–Teller distortions are not randomly distributed among the three equivalent S_4 directions, but rather the crystal presents preferential directions for distortions. According to the data of table 1, the preferential direction for this crystal would be near e_1. This result resembles the experimental observations in isomorphous A_2CuCl_4 compounds where $CuCl_4^{2-}$ is known to distort along e_1. This direction coincides with one of the S_4 axes of the inorganic BCl_4^{2-} tetrahedra in A_2BCl_4 crystals with A = Cs and TMA, and B = Zn, Co, Fe, Ni and Mn^{2+} [26, 34–36, 40]. The differences between the $\cos^2\theta_i$ and those for e_1 (table 1) might be reconciled if $CuCl_4^{2-}$ were rotated 30°, either clockwise or counterclockwise, around c. This would reflect the orientational disorder of $MnCl_4^{2-}$ in this crystal though the angle is larger for $CuCl_4^{2-}$ in TMA_2MnCl_4, than those measured for $NiCl_4^{2-}$ and $FeCl_4^{2-}$ ($\pm 8°$) in TMA_2NiCl_4 and TMA_2FeCl_4 [36].

Furthermore, the Cu^{2+} ions occupy the Mn^{2+} (4c) sites with the same probability as is deduced from the variation of the C band intensity with the polarization angle, given in the inset of figure 1. For such a situation the intensity is given by equation (4)

$$Ir^C(\varphi_{c-a}) \propto \tfrac{1}{8} \sum_{i=-4}^{4} |e_1^i \cdot (\cos \varphi_{c-a} u_c + \sin \varphi_{c-a} u_a)|^2 \tag{4}$$

where e_1^i denotes the unitary vectors along the z-axis of the $CuCl_4^{2-}$ rotated $\pm 30°$ around c (e_1^i and e_1^{-i}) in each (4c) site, $i = 1, 2, 3$ and 4. A similar equation is obtained for $Ir^C(\varphi_{c-b})$ by replacing the unitary vectors along a, u_a, and along c, u_c, by the corresponding u_b and u_c, respectively. Then, the relative intensity becomes

$$\begin{aligned} Ir^C(\varphi_{c-a}) &= 0.31 \cos^2 \varphi_{c-a} + 0.17 \sin^2 \varphi_{c-a} \\ Ir^C(\varphi_{c-b}) &= 0.31 \cos^2 \varphi_{c-b} + 0.52 \sin^2 \varphi_{c-b} \end{aligned} \tag{5}$$

in the (010) and (100) crystal faces, respectively, as was represented in the inset of figure 1.

Concerning the degree of the Jahn–Teller distortion of these $CuCl_4^{2-}$ complexes we have estimated the trans-Cl–Cu–Cl angle to be 124°, as is demonstrated in the next section.

5.2. *Charge transfer band assignment*

Within the $CuCl_4^{2-}$ (D_{2d} symmetry) MO framework, there are nine possible CT transitions involving electronic jumps from occupied mainly ligand MOs (made up of eight $3p_\pi$ and

four $3p_\sigma$ Cl^- atomic orbitals) to the unpaired mainly Cu^{2+} $b_2(\sim d(x^2-y^2))$ MO. Six of them, transforming as $a_2 + 2e + b_2 + b_1 + a_1$ irreps., have predominantly π-character and three, mainly σ, transform as $e + b_2 + a_1$ (figure 5). Only five transitions are electric dipole symmetry allowed, $e \rightarrow b_2$ and $a_1 \rightarrow b_2$ being x, y- and z-polarized, respectively.

The difficulty in making an unambiguous assignment of CT bands of $CuCl_4^{2-}$ (D_{2d}) results from the fact that only four of these five allowed transitions are clearly observed in the spectra.

This assignment in Cs compounds was made by means of the Xα calculation technique. This way, reliable MS-Xα calculations were performed by Bencini and Gatteschi [10] for explaining the CT spectra of Cs_2CuCl_4. Their procedure was similar to that outlined in section 3, but they employed greater sphere radii: $\rho(Cu) = 1.38$ Å and $\rho(Cl) = 1.62$ Å. These results lead to a virial ratio, $v_r = 0.999874$ and the CT assignment given in table 2. It is worth mentioning that these calculations predict reasonably well the energy difference between any two CT bands in the spectrum but all transitions appear shifted by about 7000 cm^{-1} (30%) to higher energies. This calculation was not able to explain successfully the z-polarized component displayed by the CT band of Cs_2CuCl_4 at 34 500 cm^{-1} which was assigned to the $3a_1 \rightarrow 4b_2$ CT transition. Following their assignment method, such a $3a_1 \rightarrow 4b_2$ transition should appear in the spectrum about 3000 cm^{-1} above the one at 24 800 cm^{-1}.

Earlier MS-Xα calculations performed by Solomon *et al* [5] in the same system, using a ratio of the sphere radii $r = 0.96$, predict CT transition energies for the Cs_2CuCl_4 system which are shifted about 9000 cm^{-1} from the experimental values, but to lower energies. The virial ratio, v_r, obtained in these calculations was 1.000 434. Later MS-Xα results by Solomon *et al* [11, 12] employing a different procedure, led to transition energies closer to the experimental values (15%). However, such a procedure which matches the potentials of the atomic spheres measured at the sphere boundaries, gave counter-intuitive values of the sphere radii: $\rho(Cu) = 1.65$ Å and $\rho(Cl) = 1.32$ Å. The radii ratio $r = 1.25$ is hard to conciliate with the ionic radii one of Cu^{2+} (or even Cu^+) and Cl^-.

Up to now, the best agreement between experimental and calculated CT transition energies has recently been obtained by Deeth [13] using the DV-Xα method. Energy differences going from 3000 cm^{-1} to 5000 cm^{-1} were obtained by this method.

In the present case of $TMA_2MnCl_4:Cu^{2+}$, the well defined polarization of the CT bands allows us to clarify their assignment. According to the previous Xα calculations, the A and B bands would correspond to $4e \rightarrow 4b_2$ and $2e \rightarrow 4b_2$ transitions, and C and C' to $2a_1 \rightarrow 4b_2$ and $3a_1 \rightarrow 4b_2$, respectively. However, following the trends of such predictions at $\theta = 129.2°$, the C' band would correspond to the $3e \rightarrow 4b_2$ transition instead of the $3a_1 \rightarrow 4b_2$ which would be located nearer the A band. This could be explained qualitatively by taking into account the fact that the oscillator strength of the $3e \rightarrow 4b_2$ transition may be weaker than that of the $3a_1 \rightarrow 4b_2$ because the 3e MO comes from the even e_g MO in the D_{4h} square planar $CuCl_4^{2-}$ complex ($\theta = 180°$) where only $e_u \rightarrow b_{1g}$ and $a_{1u} \rightarrow b_{1g}$ transitions are symmetry allowed. Therefore, it is reasonable to expect weak intensities for this transition in other $CuCl_4^{2-}$ complexes having different values of the distortion angle, θ.

In an attempt to interpret these experimental results, new MS-Xα calculations were performed in order to study the influence of θ on the CT and CF transition energies. This study was suggested by the redshift displayed by the CT bands in $TMA_2MnCl_4:Cu^{2+}$ with respect to those in TMA_2CuCl_4 and Cs_2CuCl_4 ($\theta = 129.2°$), probably due to a smaller value of θ in the former case. This assumption was confirmed by the high-energy CF band whose peak energy is known to vary linearly with θ, in the range 125° to

Table 2. Charge transfer (CT) transition assignment of $CuCl_4^{2-}$ in TMA_2MnCl_4 and Cs_2CuCl_4. The highest energy $4a_1 \rightarrow 4b_2$ crystal field (CF) transition is also included. CT transition energy differences with respect to the $4e \rightarrow 4b_2$ one are given in parentheses. *f* denotes the experimental oscillator strength. Energies are in cm^{-1}.

Transition	Type	Cs_2CuCl_4 Experimental[a]	MS-Xα			$TMA_2MnCl_4:Cu^{2+}$	
			$\theta = 129.2°$[b]	$\theta = 129.2°$[c]	$\theta = 120°$[c]	Experimental[c]	f[c]
$4a_1 \rightarrow 4b_2$	CF	*9050*	*9962*	*10 500*	*8420*	*8200*	—
$1a_2 \rightarrow 4b_2$	CT	23 000	30 558	26 410	25 680	—	—
$4e \rightarrow 4b_2$	CT	24 800 (0)	31 967 (0)	27 500 (0)	26 360 (0)	24 300 (0)	0.022 (A)
$3a_1 \rightarrow 4b_2$	CT	34 500 (9700)	34 602 (2635)	30 500 (3000)	30 320 (3960)	~29 500 (5200)	<0.001 (C')
$3e \rightarrow 4b_2$	CT	29 000 (4200)	35 794 (3827)	31 800 (4300)	30 150 (3790)	—	—
$2e \rightarrow 4b_2$	CT	34 000 (9200)	41 567 (9600)	36 100 (8600)	34 480 (8120)	33 700 (9400)	0.073 (B)
$2a_1 \rightarrow 4b_2$	CT	42 400 (17 600)	49 210 (17 243)	44 200 (16 700)	43 800 (17 440)	41 000 (16 700)	0.049 (C)

[a] Experimental data from Ferguson [7] and assignment from [10].
[b] Bencini [10].
[c] Present work.

140° [3, 4, 41], as $E(cm^{-1}) = 140\,\theta - 9240$. We detected this CF band at 8200 cm^{-1} in $TMA_2MnCl_4:Cu^{2+}$, which would correspond to a $CuCl_4^{2-}$ distortion angle $\theta = 124°$.

Table 2 shows the results of our MS-Xα calculations performed for the two $CuCl_4^{2-}$ geometries: $\theta = 129.2°$ and 120°, with the same value of $R = 2.230$ Å.

The following conclusions can be drawn: (i) for $\theta = 129.2°$, our SCF MS-Xα procedure reproduces the experimental results of Cs_2CuCl_4 more accurately than in previous calculations. The calculated CT transition energies are within 10% of the experimental values. (ii) CT bands shift to lower energies with decreasing θ; a blueshift ratio $\Delta E/\Delta\theta = 127\ cm^{-1}/deg$ is obtained for the $4e \rightarrow 4b_2$ CT transition in this θ range. This figure may explain the experimental variations found when passing from Cs_2CuCl_4 or TMA_2CuCl_4 with $\theta = 129.2°$ (~25000 cm^{-1}) [1, 7] to $(NPhpipzH_2)CuCl_4$ with $\theta = 142°$ [41] and (Bis-dipropylammonium)$CuCl_4$ with $\theta = 147°$ [4], which peak at 27 030 and 26 100 cm^{-1}, respectively. In our case, the first CT band (A) is placed 500 cm^{-1} below the corresponding one in Cs_2CuCl_4, supporting the value $\theta = 124°$. (iii) When θ decreases from 129° to 120°, the $3a_1 \rightarrow 4b_2$ transition energy also decreases, but more slowly than that of $3e \rightarrow 4b_2$. The $3a_1 \rightarrow 4b_2$ transition energy is greater than that of $3e \rightarrow 4b_2$ for $\theta = 120°$. This result may explain the observation of the C′ band placed 5200 cm^{-1} above the A band. Moreover, the $3e \rightarrow 4b_2$ and $3a_1 \rightarrow 4b_2$ transitions would have similar energies at $\theta = 124°$ and thus would appear close together in the spectrum. The fact that C′ is mainly z-polarized would reflect a higher electric dipole oscillator strength for the $3a_1 \rightarrow 4b_2$ transition than for the $3e \rightarrow 4b_2$ one at $\theta = 124°$. A general study on both the transition energy and the oscillator strength variations with the distortion angle θ and the ligand–metal distance in $CuCl_4^{2-}$ (D_{2d}) are currently under investigation.

The oscillator strengths of CT bands A, B and C were calculated from the spectra of figure 1 through the equation [42]

$$f = 3.89 \times 10^{-8}[n/(n^2 + 2)^2] \int \varepsilon \, dE \tag{6}$$

where $n = 1.5$ is the refractive index; the integral extends over the whole band, ε being the molar extinction coefficient and E, the transition energy in cm^{-1}.

The values of f calculated from equation (6) are given in table 2. The oscillator strengths $f_A = 0.022$ and $f_B = 0.073$ obtained for the x,y-polarized bands, and $f_C = 0.049$ and $f_{C'} < 0.001$ for the z-polarized bands confirm the mainly π-character of A and C′ transitions, and the mainly σ-nature of B and C, respectively.

5.3. Influences of the structural phase transition

The abrupt change of CT band intensities at $T = 171$ K, observed in figure 2, gives evidence of reorientational motions of $CuCl_4^{2-}$ induced by the $P112_1/n \rightarrow P12_1/c1$ structural phase transition. Such reorientations may be associated with both the formation of a new crystallographic phase and the existence of structural domains. This latter possibility was recently proposed to explain the optical properties of pure TMA_2MnCl_4 crystals [20, 21]. In the present work, the observation of the different CT spectra along the c-direction depending on whether the incident light was perpendicular to (100) or (010) face (figure 3) clearly indicates that we are not dealing with a single structural domain but with a domain distribution which must be different for (100) and (010) type crystals. Furthermore, below 171 K the spectrum becomes isotropic in the (010) face since it does not change when rotating the polarization plane around the incident b-axis. This isotropy indicates that the domain distribution involves $CuCl_4^{2-}$

orientations whose distortion z-axis present identical projections along the c- and a-directions.

Direct evidence of the existence of these domains was obtained by observing one (010) crystal face under crossed polarizers. The phase transition at 171 K was easily detected by such an optical configuration as the crystal became illuminated below 171 K with crossed polarizers along the extinction directions of the previous $P112_1/n$ phase. Two different domains showing extinctions at angles of 30° and 60° with the c-direction were identified. These parallelepiped shape domains with edges parallel to c and a, were almost randomly distributed. The domain distribution changed in every heating–cooling cycle around the phase transition temperature.

The analysis of CT band intensities at 10 K suggests that besides forming domains, the $CuCl_4^{2-}$ reorientates. Assuming that only two types of domains exist, the $CuCl_4^{2-}$ distortion direction, z, would lie preferentially in (100) planes for one of them. These $CuCl_4^{2-}$ orientations allow us to explain the intensities of the CT bands in the 10 K spectra: x,y-polarized bands, A and B, display similar intensities in both (100) and (010) faces along c, while the C intensity in (100) face is twice that in (010).

Finally, the present results point out the necessity of carefully verifying the possibility of a domain structure when performing polarized spectroscopic measurements at low temperatures of $CuCl_4^{2-}$ in A_2BCl_4-type crystals, most of which are known to experience structural phase transitions.

6. Conclusions

The CT spectra of $CuCl_4^{2-}$ in TMA_2MnCl_4 are explained in terms of regular D_{2d} symmetry. The CT band assignment is clarified by performing reliable polarization measurements and by correlating their energies with the theoretical MS-Xα results.

The Jahn–Teller distortion of the $CuCl_4^{2-}$ complexes takes place along preferential directions of the lattice corresponding to rotations of 30° around c with respect to that displayed by $CuCl_4^{2-}$ in pure isomorphous A_2CuCl_4 crystals. The Cl–Cu–Cl distortion angle was estimated to be 124°.

The CT spectra experience notable changes on passing the monoclinic $P112_1/n \rightarrow P12_1/c1$ phase transition temperature at $T = 171$ K. These changes were interpreted in terms of domain formation and also reorientation of the $CuCl_4^{2-}$ complexes.

Acknowledgments

Thanks are due to A G Breñosa for helping us with the crystal growing. This work has been supported by the CICYT (Project No. PB86-0304).

References

[1] Smith D W 1976 *Coord. Chem. Rev.* **21** 93
[2] Halvorson K E, Patterson C and Willet R D 1990 *Acta Crystallogr.* B **46** 508
[3] Harlow R L, Wells W J, Watt G W and Simonsen S H 1974 *Inorg. Chem.* **13** 2106
[4] Bond M R, Johnson T J and Willet R D 1988 *Can. J. Chem.* **66** 963
[5] Desjardins S R, Penfield K W, Cohen S L, Musselman R L and Solomon E I 1983 *J. Am. Chem. Soc.* **105** 4591

[6] Solomon E I 1984 *Comment. Inorg. Chem.* **3** 227
[7] Ferguson J 1964 *J. Chem. Phys.* **40** 3406
[8] Sharnoff M and Reimann C W 1967 *J. Chem. Phys.* **46** 2634
[9] Deeth R J, Hitchman M A, Lehmann G and Sachs H 1984 *Inorg. Chem.* **23** 1310
[10] Bencini A and Gatteschi D 1983 *J. Am. Chem. Soc.* **105** 5535
[11] Gewirth A A, Cohen S L, Schugar H I and Solomon E I 1987. *Inorg. Chem.* **26** 1133
[12] Gewirth A A and Solomon E I 1988 *J. Am. Chem. Soc.* **110** 3811
[13] Deeth R J 1990 *J. Chem. Soc. Dalton Trans.* 355
[14] Melia T P and Merrifield R 1970 *J. Inorg. Nucl. Chem.* **32** 1873
[15] Shimizu H, Abe N, Yasuda N, Fujimoto S, Sawada S and Shiroishi Y 1979 *Japan. J. Appl. Phys.* **18** 857
[16] Mashiyama H and Tanisaki S 1981 *J. Phys. Soc. Japan* **50** 1413
[17] Gesi K and Ozawa K 1984 *J. Phys. Soc. Japan* **53** 627
[18] Volkh O G, Kaminskii B V, Polovinko I I and Sveleba S A 1988 *Sov. Phys.–Solid State* **30** 152
[19] Zubillaga J, López-Echarri A and Tello M J 1988 *J. Phys. C: Solid State Phys.* **22** 4417
[20] Marco de Lucas M C and Rodríguez F 1989 *J. Phys.: Condens. Matter* **1** 4251
[21] Marco de Lucas M C, Rodríguez F and Moreno M 1990 *Ferroelectrics* **109** 21
[22] Breñosa A G, Moreno M and Rodríguez F 1987 *Solid State Commun.* **63** 543
[23] Breñosa A G, Rodríguez F and Moreno M 1988 *J. Phys. C: Solid State Phys.* **21** L623
[24] Breñosa A G, Rodríguez F and Moreno M 1990 *Ferroelectrics* **106** 187
[25] Johnson K H 1973 *Adv. Quantum Chem.* **7** 143
[26] Helmholz L and Kruh R F 1952 *J. Am. Chem. Soc.* **74** 1176
[27] McGinnety J A 1972 *J. Am. Chem. Soc.* **94** 8406
[28] Norman J G 1976 *Mol. Phys.* **31** 1191
[29] Aramburu J A and Moreno M 1989 *J. Chim. Phys.* **86** 871
[30] Aramburu J A, Moreno M and Bencini A 1987 *Chem. Phys. Lett.* **140** 462
[31] Aramburu J A and Moreno M 1985 *J. Chem. Phys.* **83** 6071
[32] Sturge M D 1967 *Solid State Phys.* **20** 91
[33] Willet R D, Liles O L and Michelson C 1967 *Inorg. Chem.* **6** 1885
[34] Morosin B and Lingafelter E C 1961 *J. Phys. Chem.* **65** 50
[35] Wiesner J R, Srivastava R C, Kennard C H L, Di Vaira M and Lingafelter E C 1967 *Acta Crystallogr.* **23** 565
[36] Kasano H and Mashiyana H 1990 *Ferroelectrics* **107** 293
[37] Bline R, Burgar M, Slak J, Rutar V and Milia F 1979 *Phys. Status Solidi* a **56** K65
[38] Sundaram C S, Ramakrishna J, Chandrasekhar K and Sastry V S 1986 *Ferroelectrics* **69** 299
[39] Arumugam S, Murthy K, Srinivasan R and Bhat S V 1987 *Phase Transitions* **9** 259
[40] Puget R, Jannin M, Perret R, Godefroy L and Godefroy G 1990 *Ferroelectrics* **107** 229
[41] Battaglia L P, Bonamartini Corradi A, Marcotrigiano G, Menabue L and Pellacani G C 1979 *Inorg. Chem.* **18** 148
[42] Griffith J S 1980 *The Theory of Transition-Metal Ions* (Cambridge: Cambridge University Press) p 57